Effect of ionic strength on the organization and dynamics of membrane-bound melittin

H. Raghuraman, Sourav Ganguly, Amitabha Chattopadhyay *

Centre for Cellular and Molecular Biology, Uppal Road, Hyderabad 500 007, India

Abstract

Melittin, a cationic hemolytic peptide, is intrinsically fluorescent due to the presence of a single functionally important tryptophan residue. We have previously shown that the sole tryptophan of melittin is localized in a motionally restricted environment in the membrane interface. We have monitored the effect of ionic strength on the organization and dynamics of membrane-bound melittin utilizing fluorescence and circular dichroism (CD) spectroscopic approaches. Our results show that red edge excitation shift (REES) of melittin bound to membranes is sensitive to the change in ionic strength of the medium. This could be attributed to a change in the immediate environment around melittin tryptophan with increasing ionic strength due to differential solvation of ions. Interestingly, the rotational mobility of melittin does not appear to be affected with change in ionic strength. In addition, fluorescence parameters such as lifetime and acrylamide quenching of melittin indicate an increase in water penetration in the membrane interface upon increasing ionic strength. Our results suggest that the solvent dynamics and water penetration in the interfacial region of the membranes are significantly affected at physiologically relevant ionic strength. These results assume significance in the overall context of the influence of ionic strength in the organization and dynamics of membrane proteins and membrane-active peptides.
© 2006 Elsevier B.V. All rights reserved.

Keywords: Lipid–protein interaction; Melittin organization; Red edge excitation shift; Tryptophan fluorescence; Ionic strength; Acrylamide quenching

1. Introduction

Melittin, the principal toxic component in the venom of the European honey bee, *Apis mellifera*, is a cationic hemolytic peptide [1]. It is a small linear peptide composed of 26 amino acids (NH_2-GIGAVLKVLTTGLPALISWIKRKRQQ-$CONH_2$) in which the amino-terminal region (residues 1–20) is predominantly hydrophobic whereas the carboxy-terminal region (residues 21–26) is hydrophilic due to the presence of a stretch of positively charged amino acids. This amphiphilic property of melittin makes it water soluble and yet it spontaneously associates with natural and artificial membranes [2,3]. Such a sequence of amino acids, coupled with its amphiphilic nature, is characteristic of many membrane-bound peptides and putative transmembrane helices of membrane proteins [2,4]. This has resulted in melittin being used as a convenient model for monitoring lipid–protein interactions in membranes. Apart from its powerful hemolytic activity, melittin causes bilayer micellization and membrane fusion and has also been reported to form voltage-dependent ion channels across planar lipid bilayers [2,5].

Melittin adopts predominantly random coil conformation as a monomer in aqueous solution [6]. However, at high ionic strength, pH or peptide concentration, it self-associates to form an α-helical tetrameric structure driven by the formation of a hydrophobic core [2,6]. Interestingly, melittin adopts an α-helical conformation when bound to membranes of varying lipid composition [2,7–11] or membrane-mimetic systems [12,13]. Despite the availability of a high resolution crystal structure of tetrameric melittin in aqueous solution [14], the structure of the membrane-bound form is not yet resolved by X-ray crystallography. Yet, the importance of the membrane-bound form stems from the observation that the amphiphilic α-helical conformation of this hemolytic toxin in membranes

resembles those of apolipoproteins and peptide hormones [15,16], signal peptides [17] and the envelope glycoprotein gp41 from the human immunodeficiency virus (HIV) [18]. Furthermore, understanding melittin-membrane interaction assumes greater significance due to the observation that melittin mimics the N-terminal of HIV-1 virulence factor Nef1-25 [19].

Melittin is intrinsically fluorescent due to the presence of a single tryptophan residue, Trp-19, which makes it a sensitive probe to study the interaction of melittin with membranes and membrane-mimetic systems [9–13,20–22]. This is particularly advantageous since there are no other aromatic amino acids in melittin and this makes interpretation of fluorescence data less complicated due to lack of interference and heterogeneity. More importantly, it has been shown that the sole tryptophan residue of melittin is crucial for its powerful hemolytic activity since a dramatic reduction in activity is observed upon photooxidation [23] and substitution by leucine [24]. This is further reinforced by studies with single amino acid omission analogues of melittin [25]. These reports point out the crucial role played by the uniquely positioned tryptophan in maintaining the structure and hemolytic activity of melittin. The organization and dynamics of the tryptophan residue therefore are important for the function of the peptide. We have previously monitored the microenvironment experienced by the sole tryptophan residue in melittin when bound to membranes utilizing the wavelength-selective fluorescence approach [9–11,26] and showed that the tryptophan residue is located in a motionally restricted interfacial region of the membrane. These results are consistent with earlier reports which showed that the tryptophan residues of membrane peptides and proteins tend to be preferentially localized at the membrane interface [27,28].

Melittin has been widely used as a suitable model peptide for studying lipid–protein interactions due to its various modes of action with natural and model membranes [2,5]. It is well documented that the orientation (parallel or perpendicular to the plane of the membrane bilayer) and the lytic activity of melittin are dependent on the physical condition and the composition of the membrane to which it is bound [8–10,29–31]. In this paper, we have monitored the effect of ionic strength on the organization and dynamics of melittin bound to DOPC membranes utilizing fluorescence and circular dichroism (CD) spectroscopic approaches. Our results suggest that the solvent dynamics and water penetration in the interfacial region of the membrane around the tryptophan residue of melittin are significantly affected at physiologically relevant ionic strengths, which assume significance in the overall context of the role of ionic strength in the organization and function of membrane proteins and membrane-active peptides.

2. Materials and methods

2.1. Materials

Melittin of the highest available purity and MOPS were obtained from Sigma Chemical Co. (St. Louis, MO, U.S.A.). DOPC and DMPC were purchased from Avanti Polar Lipids (Alabaster, AL, U.S.A.). Lipids were checked for purity by thin layer chromatography on silica gel precoated plates (Sigma) in chloroform/methanol/water (65:35:5, v/v/v) and were found to give only one spot in all cases with a phosphate-sensitive spray and on subsequent charring [32]. The concentration of DOPC was determined by phosphate assay subsequent to total digestion by perchloric acid [33]. DMPC was used as an internal standard to assess lipid digestion. The concentration of melittin in aqueous solution was calculated from its molar extinction coefficient (ε) of 5570 M^{-1} cm^{-1} at 280 nm [9]. Ultrapure grade acrylamide was from Invitrogen Life Technologies (Carlsbad, CA, U.S.A.). The purity of acrylamide was checked from its absorbance using its molar extinction coefficient (ε) of 0.23 M^{-1} cm^{-1} at 295 nm and optical transparency beyond 310 nm [34]. All other chemicals used were of the highest purity available. The solvents used were of spectroscopic grade. Water was purified through a Millipore (Bedford, MA, U.S.A.) Milli-Q system and used throughout.

2.2. Sample preparation

All experiments were done using small unilamellar vesicles (SUVs) containing 1 mol% melittin. In general, 640 nmol (320 nmol for fluorescence quenching experiments and 2560 nmol for CD measurements) lipid was dried under a stream of nitrogen while being warmed gently (∼ 35 °C). After further drying under a high vacuum for more than 3 h, 1.5 ml of 10 mM MOPS, 5 mM EDTA, pH 7.2 buffer containing various concentrations of sodium chloride was added, and the sample was vortexed for 3 min to disperse the lipid and form homogeneous multilamellar vesicles. The lipid dispersions were then sonicated using Branson model 250 sonifier (Danbury, CT) fitted with a microtip until they were clear (∼ 20 min in the presence of argon while being cooled in ice) to form SUVs. The sonicated samples were then centrifuged at 13,000 rpm for 10 min to remove any titanium particle shed from the microtip during sonication. To incorporate melittin into membranes, 6.4 nmol (3.2 nmol and 25.6 nmol for quenching and CD measurements, respectively) of melittin was added from a stock solution in water to the pre-formed vesicles and mixed well. The samples were incubated in dark for 12 h at room temperature (∼ 23 °C) for equilibration before making measurements. Background samples were prepared the same way except that melittin was not added to them. All experiments were done at room temperature (∼ 23 °C).

2.3. Steady state fluorescence measurements

Steady state fluorescence measurements were performed with a Hitachi F-4010 spectrofluorometer (Tokyo, Japan) using 1 cm path length quartz cuvettes. Excitation and emission slits with a nominal bandpass of 5 nm were used for all measurements. All spectra were recorded using the correct spectrum mode. Background intensities of samples in which melittin was omitted were subtracted from each sample spectrum to cancel out any contribution due to the solvent Raman peak and other scattering artifacts. In cases of excitation >300 nm, the sample was scanned more than

once (generally three times) and the signal was averaged to improve signal-to-noise ratio. In these cases, the sample was checked at the end of the experiment for any possible photodamage induced by repeated scanning. We did not observe any photodamage to the samples under these conditions. The spectral shifts obtained with different sets of samples were identical in most cases. In other cases, the values were within ±1 nm of the ones reported. Fluorescence anisotropy measurements were performed at room temperature (∼23 °C) using a Hitachi polarization accessory. Anisotropy values were calculated from the equation [35]:

$$r = \frac{I_{\mathrm{VV}} - GI_{\mathrm{VH}}}{I_{\mathrm{VV}} + 2GI_{\mathrm{VH}}} \tag{1}$$

where I_{VV} and I_{VH} are the measured fluorescence intensities (after appropriate background subtraction) with the excitation polarizer vertically oriented and emission polarizer vertically and horizontally oriented, respectively. G is the grating correction factor and is the ratio of the efficiencies of the detection system for vertically and horizontally polarized light, and is equal to $I_{\mathrm{HV}}/I_{\mathrm{HH}}$. All experiments were done with multiple sets of samples and average values of anisotropy are shown in Fig. 2.

2.4. Time-resolved fluorescence measurements

Fluorescence lifetimes were calculated from time-resolved fluorescence intensity decays using a Photon Technology International (London, Western Ontario, Canada) LS-100 luminescence spectrophotometer in the time-correlated single photon counting mode. This machine uses a thyratron-gated nanosecond flash lamp filled with nitrogen as the plasma gas (16±1 in. of mercury vacuum) and is run at 18–20 kHz. Lamp profiles were measured at the excitation wavelength using Ludox (colloidal silica) as the scatterer. To optimize the signal-to-noise ratio, 10,000 photon counts were collected in the peak channel. All experiments were performed using excitation and emission slits with a bandpass of 6 nm or less. The sample and the scatterer were alternated after every 5% acquisition to ensure compensation for shape and timing drifts occurring during the period of data collection. This arrangement also prevents any prolonged exposure of the sample to the excitation beam thereby avoiding any possible photodamage of the fluorophore. The data stored in a multichannel analyzer was routinely transferred to an IBM PC for analysis. Fluorescence intensity decay curves so obtained were deconvoluted with the instrument response function and analyzed as a sum of exponential terms:

$$F(t) = \Sigma_i \alpha_i \exp(-t/\tau_i) \tag{2}$$

where $F(t)$ is the fluorescence intensity at time t and α_i is a pre-exponential factor representing the fractional contribution to the time-resolved decay of the component with a lifetime τ_i such that $\Sigma_i\alpha_i = 1$. The decay parameters were recovered as described previously [12]. Mean (average) lifetimes $\langle\tau\rangle$ for

biexponential decays of fluorescence were calculated from the decay times and pre-exponential factors using the following equation [35]:

$$\langle\tau\rangle = \frac{\alpha_1\tau_1^2 + \alpha_2\tau_2^2}{\alpha_1\tau_1 + \alpha_2\tau_2} \tag{3}$$

2.5. Fluorescence quenching measurements

Acrylamide quenching experiments of melittin tryptophan fluorescence in membranes containing various concentrations of sodium chloride were carried out by measurement of fluorescence intensity of melittin after serial addition of small aliquots of a freshly prepared stock solution of 8 M acrylamide in water to the sample while being stirred followed by incubation for 2 min in the sample compartment in the dark (shutters closed). The excitation wavelength used was 295 nm and emission was monitored at 336 nm. Corrections for inner filter effect were made using the following equation [35]:

$$F = F_{\mathrm{obs}}\mathrm{antilog}[(A_{\mathrm{ex}} + A_{\mathrm{em}})/2] \tag{4}$$

where F is the corrected fluorescence intensity and F_{obs} is the background subtracted fluorescence intensity of the sample. A_{ex} and A_{em} are the measured absorbance at the excitation and emission wavelengths. The absorbance of the samples was measured using a Hitachi U-2000 UV–visible absorption spectrophotometer. Quenching data were analyzed by fitting to the Stern-Volmer equation [35]:

$$F_{\mathrm{o}}/F = 1 + K_{\mathrm{SV}}[Q] = 1 + k_{\mathrm{q}}\tau_{\mathrm{o}}[Q] \tag{5}$$

where F_{o} and F are the fluorescence intensities in the absence and presence of the quencher, respectively, $[Q]$ is the molar quencher concentration and K_{SV} is the Stern-Volmer quenching constant. The Stern-Volmer quenching constant K_{SV} is equal to $k_{\mathrm{q}}\tau_{\mathrm{o}}$ where k_{q} is the bimolecular quenching constant and τ_{o} is the lifetime of the fluorophore in the absence of quencher.

2.6. Circular dichroism measurements

CD measurements were carried out at room temperature (∼23 °C) on a JASCO J-715 spectropolarimeter which was calibrated with (+)-10-camphorsulfonic acid [36]. The spectra were scanned in a quartz optical cell with a path length of 0.1 cm. All spectra were recorded in 0.2 nm wavelength increments with a 4 s response and a bandwidth of 1 nm. For monitoring changes in secondary structure, spectra were scanned in the far-UV range from 205 to 250 nm at a scan rate of 50 nm/min. Each spectrum is the average of 15 scans with a full scale sensitivity of 50 mdeg. All spectra were corrected for background by subtraction of appropriate blanks and were smoothed making sure that the overall shape of the spectrum remains unaltered. Data are represented as molar ellipticities and were calculated using the equation:

$$[\theta] = \theta_{\mathrm{obs}}/(10Cl) \tag{6}$$

where θ_{obs} is the observed ellipticity in mdeg, l is the path length in cm and C is the melittin concentration in mol/l.

3. Results

3.1. Red edge excitation shift of membrane-bound melittin

Red edge excitation shift (REES) represents a powerful approach which can be used to directly monitor the environment and dynamics around a fluorophore in a complex biological system [37,38]. A shift in the wavelength of maximum fluorescence emission toward higher wavelengths, caused by a shift in the excitation wavelength toward the red edge of the absorption band, is termed REES. This effect is mostly observed with polar fluorophores in motionally restricted media such as viscous solutions or condensed phases where the dipolar relaxation time for the solvent shell around a fluorophore is comparable to or longer than its fluorescence lifetime [37–39]. REES arises from slow rates of solvent relaxation (reorientation) around an excited state fluorophore which depends on the motional restriction imposed on the solvent molecules in the immediate vicinity of the fluorophore. Utilizing this approach, it becomes possible to probe the mobility parameters of the environment itself (which is represented by the relaxing solvent molecules) using the fluorophore merely as a reporter group. Further, since the ubiquitous solvent for biological systems is water, the information obtained in such cases will come from the otherwise 'optically silent' water molecules.

The unique feature about REES is that while all other fluorescence techniques (such as fluorescence quenching, energy transfer and anisotropy measurements) yield information about the fluorophore (either intrinsic or extrinsic) itself, REES provides information about the relative rates of solvent (water in biological systems) relaxation dynamics which is not possible to obtain by other techniques. This makes REES extremely useful since hydration plays a crucial modulatory role in a large number of important cellular events including protein folding, lipid–protein interactions and ion transport [40]. We have previously shown that REES serves as a powerful tool to monitor the organization and dynamics of fluorescent probes, peptides and proteins bound to membranes and membrane mimetic media such as micelles and reverse micelles [37,38,41–46].

Melittin is predominantly in the monomeric form in aqueous solution under the experimental conditions used by us [6]. The fluorescence emission maximum of melittin bound to DOPC membranes is 335 nm when excited at 280 nm irrespective of the presence or absence of salt in the buffer used to disperse the lipid (see Fig. 1b). The magnitude of the emission maximum is indicative of the membrane interfacial localization of the tryptophan residue in melittin [9,10,26]. The shifts in the maxima of fluorescence emission[1] of the tryptophan residue of

---

[1] We have used the term maximum of fluorescence emission in a somewhat wider sense here. In every case, we have monitored the wavelength corresponding to maximum fluorescence intensity, as well as the center of mass of the fluorescence emission. In most cases, both these methods yielded the same wavelength. In cases where minor discrepancies were observed, the center of mass of emission has been reported as the fluorescence maximum.
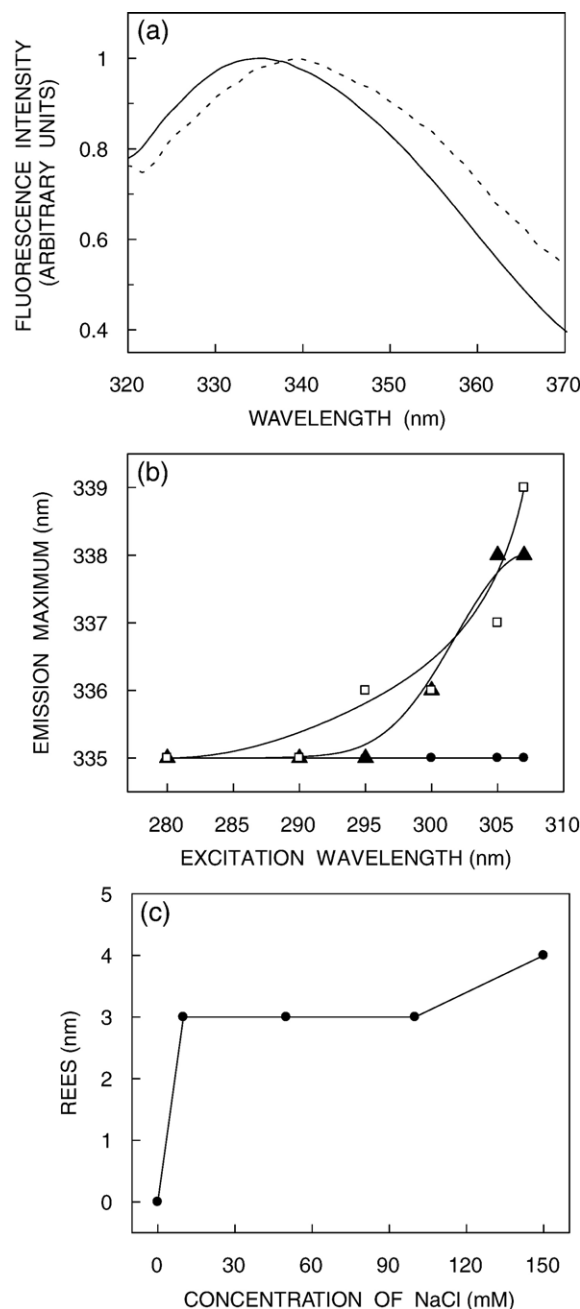

Fig. 1. (a) Representative fluorescence emission spectra of membrane-bound melittin in presence of 150 mM NaCl as a function of increasing excitation wavelength corresponding to 280 (——) and 307 (-----) nm. The spectra are intensity-normalized at the emission maximum. (b) Effect of changing excitation wavelength on the wavelength of maximum emission of melittin bound to DOPC membranes under conditions of increasing ionic strength corresponding to 0 (●), 10 (▲) and 150 (□) mM NaCl. (c) Effect of increasing ionic strength on the magnitude of REES of membrane-bound melittin. REES data obtained from Fig. 1b is plotted as a function of increasing salt concentration. The ratio of melittin to lipid was 1:100 (mol/mol) and the concentration of melittin was 4.27 μM in all cases. See Materials and methods for other details.

melittin, bound to DOPC membranes under conditions of increasing ionic strength, as a function of excitation wavelength are shown in Fig. 1b. As the excitation wavelength is changed from 280 to 307 nm, the emission maximum of membrane-bound melittin remains invariant in the absence of NaCl. This

implies that melittin bound to DOPC membranes displays no REES in the absence of added salt. Interestingly, the emission maxima of membrane-bound melittin shift from 335 to 338 nm and 335 to 339 nm for samples containing 10 and 150 mM NaCl, respectively. It is possible that there could be further red shift if excitation is carried out beyond 307 nm. We found it difficult to work in this wavelength range due to low signal-to-noise ratio and artifacts due to the solvent Raman peak that sometimes remained even after background subtraction. Such dependence of the emission maximum on excitation wavelength is characteristic of REES (see Fig. 1a and b). This implies that the tryptophan residue in melittin is localized in a motionally restricted region of the membrane in these cases. This is consistent with the recent report in which it has been shown that the hydration dynamics around the tryptophan residue of melittin slows down when bound to membranes [47]. In a broader context, this observation is in agreement with the interfacial localization of the tryptophan residue of membrane-bound melittin [9,10,26]. The membrane interface is characterized by unique motional and dielectric characteristics distinct from both the bulk aqueous phase and the more isotropic hydrocarbon-like deeper regions of the membrane [37,48]. This specific region of the membrane exhibits slow rates of solvent relaxation and is also known to participate in intermolecular charge interactions and hydrogen bonding through the polar headgroup. These structural features which slow down the rate of solvent reorientation have previously been recognized as typical features of microenvironments giving rise to significant REES effects. It is therefore the membrane interface, which is most likely to display red edge effects [37].

The effect of increasing ionic strength on the magnitude of REES of membrane-bound melittin is shown in Fig. 1c. While membrane-bound melittin does not exhibit REES in the absence of salt, it exhibits REES of 3 nm when the concentration of NaCl is very low (10 mM). The sensitivity of REES with increasing salt concentration becomes weak beyond 10 mM NaCl. Thus, membrane-bound melittin exhibits REES of 4 nm when the concentration of NaCl is increased to 150 mM. The magnitude of REES therefore appears to be critically dependent on the presence of salt only at very low salt concentration. These results show that the immediate environment around the tryptophan, in terms of dynamics of hydration (rate of solvent reorientation), changes with increasing salt concentration. This could be due to increased motional restriction of solvent dipoles around the excited state tryptophan residue caused by the solvation of ions at the membrane interface.

3.2. Fluorescence anisotropy and lifetime measurements of membrane-bound melittin

The effect of increasing ionic strength on steady state fluorescence anisotropy of melittin bound to DOPC membranes is shown in Fig. 2a. It is evident from the figure that the anisotropy values of melittin tryptophan do not show significant variation with increasing ionic strength. This indicates that the rotational mobility of melittin is not affected in a major way by the presence of salt. Importantly, this result
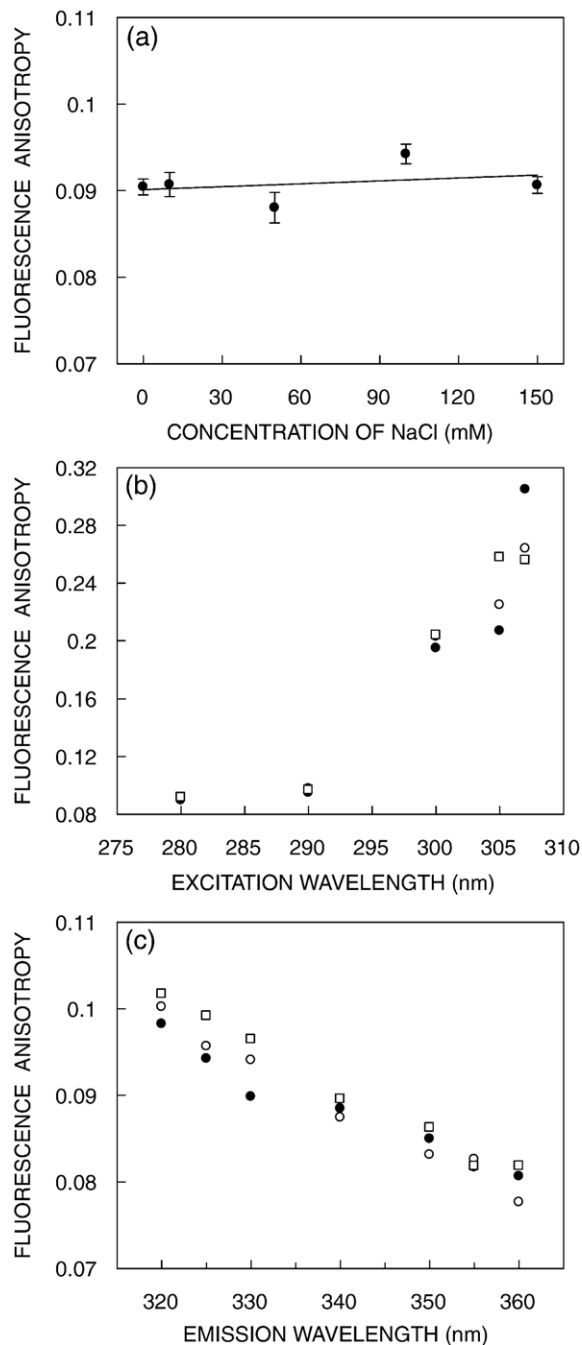

Fig. 2. (a) Effect of increasing ionic strength on the fluorescence anisotropy of membrane-bound melittin. The excitation wavelength used was 280 nm and emission was collected at 335 nm. The data points shown are the means±S.E. of three independent measurements. All other conditions are as in Fig. 1. See Materials and methods for other details. (b and c) Fluorescence anisotropy of membrane-bound melittin under conditions of increasing ionic strength corresponding to 0 (O), 10 (●) and 150 (□) mM NaCl as a function of (b) excitation and (c) emission wavelengths. Anisotropy values were recorded at 335 nm in (b). The excitation wavelength used was 280 nm in (c). The data points shown are the means of three independent measurements. All other conditions are as in Fig. 1. See Materials and methods for other details.

suggests that the binding of melittin to DOPC membranes is not affected upon increasing salt concentration (also evident from invariant fluorescence emission maximum when excited at 280 nm and CD spectra, see Figs. 1b and 6). Fluorescence
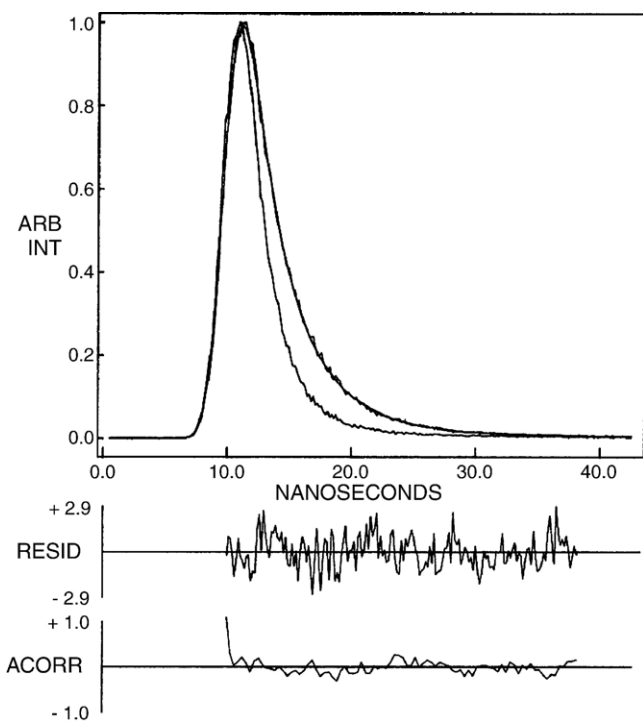
Fig. 3. Time-resolved fluorescence intensity decay of melittin bound to DOPC membranes. Excitation wavelength was 297 nm, which corresponds to a peak in the spectral output of the nitrogen lamp. Emission was monitored at 335 nm. The sharp peak on the left is the lamp profile. The relatively broad peak on the right is the decay profile, fitted to a biexponential function. The two lower plots show the weighted residuals and the autocorrelated function of the weighted residuals. All other conditions are as in Fig. 1. See Materials and methods for other details.

Table 1
Effect of ionic strength on fluorescence lifetimes of melittin bound to DOPC membranes [a]

NaCl (mM)	α_1	τ_1 (ns)	α_2	τ_2 (ns)	$\langle\tau\rangle$ (ns)
0	0.89	0.51	0.11	3.18	1.67
10	0.90	0.59	0.10	3.16	1.55
50	0.90	0.57	0.10	3.06	1.50
100	0.91	0.51	0.09	3.02	1.44
150	0.91	0.57	0.09	3.03	1.42

[a] The excitation wavelength was 297 nm; emission was monitored at 335 nm. Mean fluorescence lifetimes were calculated using Eq. (3). All other conditions are as in Fig. 1. See Materials and methods for other details.

anisotropy is also known to be dependent on excitation and emission wavelengths in motionally restricted media [49]. A plot of steady state anisotropy of membrane-bound melittin as a function of excitation wavelength is shown in Fig. 2b for different concentrations of NaCl. The extent of increase in anisotropy in all cases strengthens our earlier conclusion that melittin is localized in a motionally restricted environment and the rotational mobility of melittin is not affected upon increasing the salt content. In addition, we monitored the change in fluorescence anisotropy of melittin bound to DOPC membranes as a function of emission wavelength under these conditions (see Fig. 2c). There is a considerable reduction in fluorescence anisotropy upon increasing the emission wavelength irrespective of the presence or absence of salt. The lowest anisotropy is observed toward longer wavelengths (red edge) where emission from the relaxed fluorophores predominates. Taken together, these results suggest that the tryptophan residue of melittin experiences motional restriction when bound to DOPC membranes irrespective of the ionic strength.

Fluorescence lifetime serves as a faithful indicator of the local environment in which a given fluorophore is placed. In addition, it is well known that fluorescence lifetime of tryptophan in particular is sensitive to solvent, temperature and excited state interactions [50,51]. A typical decay profile of tryptophan residue of membrane-bound melittin with its

biexponential fitting and the various statistical parameters used to check the goodness of the fit is shown in Fig. 3. The fluorescence lifetimes of melittin bound to DOPC membranes as a function of ionic strength are shown in Table 1. As seen from the table, all fluorescence decays could be fitted well with a biexponential function. The mean fluorescence lifetimes were calculated using Eq. (3) and are shown in Table 1. As seen from the values of mean lifetime, there is a continuous decrease (~15%) in mean fluorescence lifetime of melittin with increasing salt concentration. The shortening of lifetime could possibly be due to increased water penetration in the interfacial region of membranes due to increased solvation of ions near the positively charged residues of melittin and at the membrane interface. In general, an increase in polarity of the tryptophan environment is known to reduce the lifetime of tryptophans due to fast deactivating processes in polar environments [51]. Interestingly, the change in mean fluorescence lifetime is more prominent at very low (10 mM) salt concentration, similar to the change in REES with salt concentration (Fig. 1c).

In order to ensure that the anisotropy values measured for membrane-bound melittin are not influenced by lifetime-
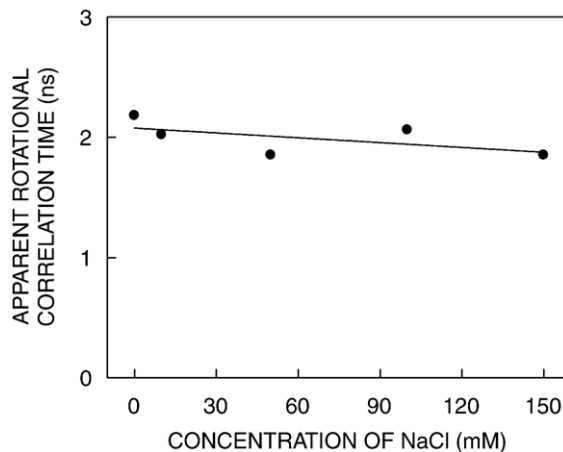

Fig. 4. Effect of increasing ionic strength on apparent rotational correlation times of membrane-bound melittin. The apparent rotational correlation times were calculated using Eq. (7). See Materials and methods, and Results for other details.

induced artifacts, the apparent (average) rotational correlation times were calculated using Perrin's equation [35]:

$$\tau_c = \frac{\langle \tau \rangle r}{r_o - r} \qquad (7)$$

where r_o is the limiting anisotropy of tryptophan, r is the steady state anisotropy and $\langle \tau \rangle$ is the mean fluorescence lifetime taken from Table 1. The values of the apparent rotational correlation times, calculated this way using a value of r_o of 0.16 [52], are shown in Fig. 4. As is evident from the figure, the apparent rotational correlation times do not show a significant change as a function of increasing ionic strength and therefore parallel the trend observed with fluorescence anisotropy of membrane-bound melittin. This clearly shows that the observed changes in anisotropy values are free from lifetime-induced artifacts. Interestingly, the relatively short apparent rotational correlation time possibly indicates that melittin is bound to the membrane interface and is not involved in pore formation.

3.3. Acrylamide quenching of melittin tryptophan fluorescence

The above results show that increasing salt concentration enhances the polarity of the interfacial region of membranes possibly due to increased water penetration. We performed fluorescence quenching experiments using acrylamide to explore this issue further and to examine the accessibility and relative location of melittin in membranes under conditions of increasing ionic strength. Acrylamide is a widely used neutral aqueous quencher of tryptophan fluorescence [53]. Representative results of these experiments for quenching of the tryptophan residue of membrane-bound melittin by acrylamide in the absence and presence of 150 mM NaCl are plotted in Fig. 5a, as Stern-Volmer plots. The slope of such a plot (K_{SV}) is related to the degree of exposure (accessibility) of the melittin tryptophan to the aqueous phase. In general, the higher the slope, the greater the degree of exposure, assuming that there is not a large difference in fluorescence lifetime. The quenching parameter (K_{SV}) obtained by analyzing the Stern-Volmer plots is shown in Fig. 5b. The K_{SV} value of melittin in DOPC membranes was found to be 1.3 M^{-1}. Addition of up to 150 mM NaCl to DOPC membranes leads to an apparent increase in the accessibility of the melittin tryptophan to acrylamide as evident from an increase in K_{SV} (see Fig. 5b). This suggests that the tryptophan residue in membrane-bound melittin, under conditions of increasing ionic strength, is more exposed to the quencher possibly as a result of increased water penetration in the membrane interfacial region. However, interpretation of K_{SV} values is complicated this way due to its intrinsic dependence on fluorescence lifetime (see Eq. (5)). The bimolecular quenching constant (k_q) is a more accurate measure of the degree of exposure since it takes into account the differences in fluorescence lifetime. The k_q values, calculated using mean fluorescence lifetimes from Table 1 and Eq. (5), are shown in Fig. 5b. The figure
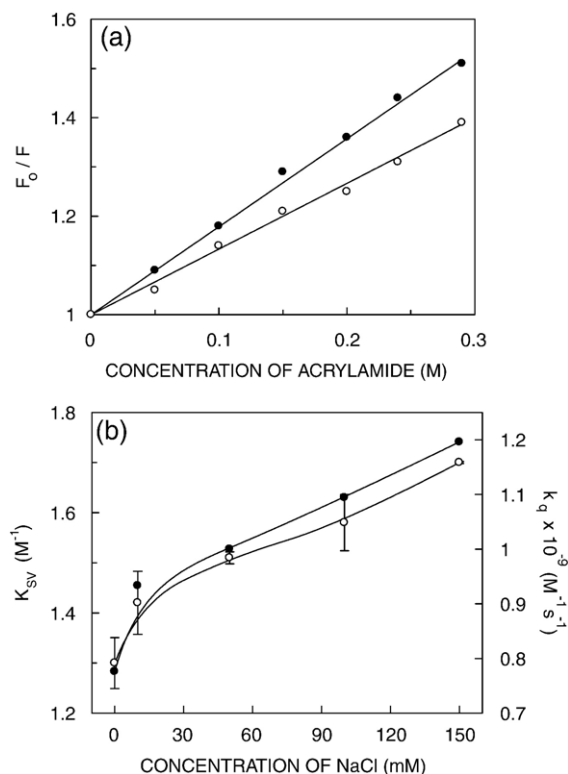

Fig. 5. (a) Representative data for Stern-Volmer analysis of acrylamide quenching of melittin fluorescence in DOPC membranes at different ionic strength conditions corresponding to 0 (○) and 150 (●) mM NaCl. F_o is the fluorescence intensity in the absence of quencher, F is the corrected fluorescence intensity in the presence of quencher. (b) Stern-Volmer quenching constants, K_{SV}, (○) and bimolecular quenching constants, k_q, (●) for acrylamide quenching of melittin bound to DOPC membranes as a function of increasing ionic strength. The bimolecular quenching constants were calculated using Eq. (5). The excitation wavelength was 295 nm and emission was monitored at 335 nm. The data points shown are the means±S.E. of three independent measurements. The ratio of melittin to lipid was 1:100 (mol/mol) and the concentration of melittin was 2.13 μM in all cases. See Materials and methods for other details.

shows that the k_q values are in overall agreement with K_{SV} values thereby reinforcing our earlier proposition that there is an increased water penetration in the interfacial region of membranes with increasing ionic strength where the sole tryptophan residue of melittin is localized. It is interesting to note again that this effect is more pronounced at very low (10 mM) salt concentration, and this is similar to the trend observed in changes in REES (Fig. 1c) and fluorescence lifetime (Table 1).

3.4. Effect of ionic strength on the secondary structure of membrane-bound melittin

To investigate the effect of ionic strength on the secondary structure of membrane-bound melittin, we carried out far-UV CD spectroscopy of melittin in membranes as a function of ionic strength. It is well established that monomeric melittin in aqueous solution shows essentially random coil conformation as reported earlier [9,10]. On the other hand, membrane-bound melittin shows a CD spectrum which is characteristic of an α-
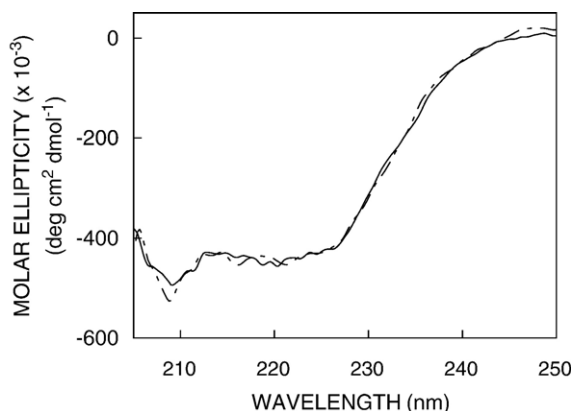
Fig. 6. Effect of increasing ionic strength on the far-UV CD spectra of membrane-bound melittin corresponding to 0 (− - −) and 150 (——) mM NaCl. The ratio of melittin to lipid was 1:100 (mol/mol) and the concentration of melittin was 17 μM in all cases. See Materials and methods for other details.

helical conformation [7–11,29,54]. The CD spectra of melittin bound to DOPC membranes containing 0 and 150 mM NaCl are shown in Fig. 6. The secondary structure of membrane-bound melittin does not appear to be sensitive to the presence of salt in the membrane.

4. Discussion

It is well known that ionic strength influences the conformation, stability and function of proteins [55,56]. The presence of salts could affect proteins in many ways. For example, salts influence the redistribution of charges close to the protein surface and induce a reorganization of water molecules which in turn could affect interaction of the protein with membranes. In addition, there could be a specific interaction between the charged amino acid residues in proteins and ions present in salts. In fact, it has recently been shown that the ionic strength-induced conformational changes on the cytolytic toxin Cyt1A is due to the specific interaction of salt ions with the charged amino acids in the protein [57]. Apart from the effect of ionic strength on protein structure, the influence of salts on the organization of membranes should also be considered in case of membrane-bound proteins and peptides. For example, increasing salt concentration has been shown to reduce diffusion of membrane lipids [58]. In addition, salts differentially affect membrane surface properties (including interfacial hydration) and membrane curvature [59] which in turn could influence lipid–protein interactions and the function of biological membranes [60].

In this paper, we have monitored the effect of ionic strength in modulating lipid–protein interactions using the membrane-bound hemolytic peptide melittin as a model peptide. We monitored the effect of increasing salt concentration on the organization and dynamics of melittin bound to DOPC membranes utilizing sensitive fluorescence-based approaches and CD spectroscopy. We chose zwitterionic phosphatidylcholine as the phospholipid headgroup in this study to ensure that there is minimal electrostatic interaction with the cationic peptide melittin. Since melittin is a hemolytic peptide and

targets the membrane from the aqueous phase, it is important to understand the effect of physical factors such as ionic strength on the organization and dynamics of membrane-bound melittin. We used NaCl to change the ionic strength of the medium since it is a neutral salt in the Hofmeister series and is at the midpoint between the stabilizing and destabilizing effects. In addition, the concentration of salt used was such that the ionic strength is in the physiological range. This would allow us to monitor the possible changes in the dynamics of membrane-bound melittin without any drastic change in protein structure.

Our results show that REES is sensitive to change in the ionic strength of the medium. Membrane-bound melittin does not show any REES in the absence of salt. Importantly, melittin exhibits REES of 4 nm at the physiologically relevant ionic strength corresponding to 150 mM NaCl. This increase in REES with ionic strength is not gradual since REES of 3 nm was observed for the lowest salt concentration (10 mM) studied. This could be attributed to differential rates of solvent reorientation around the excited state melittin tryptophan at the membrane interface in the absence and presence of salt. It should be mentioned here that monomeric melittin in aqueous solution exhibits ∼1 nm REES in presence of 150 mM NaCl (not shown). Interestingly, the rotational mobility of melittin does not appear to be affected irrespective of the presence or absence of salt, which is supported by apparent rotational correlation times. In addition, fluorescence parameters such as lifetime and acrylamide quenching of melittin indicate an increase in water penetration in the membrane interface upon increasing the salt content in buffer. Increasing ionic strength does not affect the secondary structure of membrane-bound melittin (α-helix) as determined by circular dichroism studies. Overall, our results of change in dynamics of membrane-bound melittin are attributed to an increase in water penetration and differential rates of solvent relaxation in membranes in response to change in ionic strength. These results assume significance in the overall context of the influence of ionic strength in the organization and dynamics of membrane proteins and membrane-active peptides.

Acknowledgements

References

[1] E. Habermann, Bee and wasp venoms, Science 177 (1972) 314–322.
[2] C.E. Dempsey, The actions of melittin on membranes, Biochim. Biophys. Acta 1031 (1990) 143–161.

[3] G. Saberwal, R. Nagaraj, Cell-lytic and antibacterial peptides that act by perturbing the barrier function of membranes: facets of their conformational features, structure–function correlation and membrane-perturbing abilities, Biochim. Biophys. Acta 1197 (1994) 109–131.

[4] Y. Shai, Molecular recognition between membrane-spanning polypeptides, Trends Biochem. Sci. 20 (1995) 460–464.

[5] B. Bechinger, Structure and functions of channel-forming peptides: magainins, cecropins, melittin and alamethicin, J. Membr. Biol. 156 (1997) 197–211.

[6] J. Bello, H.R. Bello, E. Granados, Conformation and aggregation of melittin: dependence on pH and concentration, Biochemistry 21 (1982) 461–465.

[7] H.H.J. De Jongh, E. Goormaghtigh, J.A. Killian, Analysis of circular dichroism spectra of oriented protein–lipid complexes: toward a general application, Biochemistry 33 (1994) 14521–14528.

[8] R. Smith, F. Separovic, T.J. Milne, A. Whittaker, F.M. Bennett, B.A. Cornell, A. Makriyannis, Structure and orientation of the pore-forming peptide, melittin, in lipid bilayers, J. Mol. Biol. 241 (1994) 456–466.

[9] A.K. Ghosh, R. Rukmini, A. Chattopadhyay, Modulation of tryptophan environment in membrane-bound melittin by negatively charged phospholipids: implications in membrane organization and function, Biochemistry 36 (1997) 14291–14305.

[10] H. Raghuraman, A. Chattopadhyay, Interaction of melittin with membrane cholesterol: a fluorescence approach, Biophys. J. 87 (2004) 2419–2432.

[11] H. Raghuraman, A. Chattopadhyay, Influence of lipid chain unsaturation on membrane-bound melittin: a fluorescence approach, Biochim. Biophys. Acta 1665 (2004) 29–39.

[12] H. Raghuraman, A. Chattopadhyay, Organization and dynamics of melittin in environments of graded hydration: a fluorescence approach, Langmuir 19 (2003) 10332–10341.

[13] H. Raghuraman, A. Chattopadhyay, Effect of micellar charge on the conformation and dynamics of melittin, Eur. Biophys. J. 33 (2004) 611–622.

[14] T.C. Terwilliger, D. Eisenberg, The structure of melittin, J. Biol. Chem. 237 (1982) 6016–6022.

[15] E.T. Kaiser, F.J. Kezdy, Secondary structures of proteins and peptides in amphiphilic environment, Proc. Natl. Acad. Sci. U. S. A. 80 (1983) 1137–1143.

[16] H.S. Morii, S. Honda, S. Ohashi, H. Uedaira, Alpha-helical assembly of biologically active peptides and designed helix bundle protein, Biopolymers 34 (1994) 481–488.

[17] C. Golding, P. O' Shea, The interactions of signal sequences with membranes, Biochem. Soc. Trans. 23 (1995) 971–976.

[18] M. Rabenstein, Y.K. Shin, A peptide from the heptad repeat of human immunodeficiency virus gp41 shows both membrane binding and coiled-coil formation, Biochemistry 34 (1995) 13390–13397.

[19] K.J. Barnham, S.A. Monks, M.G. Hinds, A.A. Azad, R.S. Norton, Solution structure of polypeptide from the N terminus of the HIV protein Nef, Biochemistry 36 (1997) 5970–5980.

[20] Y. Cajal, M.K. Jain, Synergism between melittin and phospholipase A2 from bee venom: apparent activation by intervesicle exchange of phospholipids, Biochemistry 36 (1997) 3882–3893.

[21] T.D. Bradrick, A. Philippetis, S. Georghiou, Stopped-flow fluorometric study of the interaction of melittin with phospholipid bilayers: importance of the physical state of the bilayer and the acyl chain length, Biophys. J. 69 (1995) 1999–2010.

[22] Z. Oren, Y. Shai, Selective lysis of bacteria but not mammalian cells by diastereomers of melittin: structure–function study, Biochemistry 36 (1997) 1826–1835.

[23] E. Habermann, H. Kowallek, Modifications of amino groups and tryptophan in melittin as an aid to recognition of structure–activity relationships, Hoppe-Seylers Z. Physiol. Chem. 351 (1970) 884–890.

[24] S.E. Blondelle, R.A. Houghten, Probing the relationships between the structure and hemolytic activity of melittin with a complete set of leucine substitution analogues, J. Pept. Res. 4 (1991) 12–18.

[25] S.E. Blondelle, R.A. Houghten, Hemolytic and antimicrobial activities of twenty-four individual omission analogues of melittin, Biochemistry 30 (1991) 4671–4678.

[26] A. Chattopadhyay, R. Rukmini, Restricted mobility of the sole tryptophan in membrane-bound melittin, FEBS Lett. 335 (1993) 341–344.

[27] W.M. Yau, W.C. Wimley, K. Gawrisch, S.H. White, The preference of tryptophan for membrane interfaces, Biochemistry 37 (1998) 14713–14718.

[28] M.R. de Planque, B.B. Bonev, J.A. Demmers, D.V. Greathouse, R.E. Koeppe, F. Separovic, A. Watts, J.A. Killian, Interfacial anchor properties of tryptophan residues in transmembrane peptides can dominate over hydrophobic matching effects in peptide–lipid interactions, Biochemistry 42 (2003) 5341–5348.

[29] L. Yang, T.A. Harroun, T.M. Weiss, L. Ding, H.W. Huang, Barrel-stave model or toroidal model ? A case study on melittin pores, Biophys. J. 81 (2001) 1475–1485.

[30] N.K. Subbarao, R.C. MacDonald, Lipid unsaturation influences melittin-induced leakage of vesicles, Biochim. Biophys. Acta 1189 (1994) 101–107.

[31] H. Raghuraman, A. Chattopadhyay, Cholesterol inhibits the lytic activity of melittin in erythrocytes, Chem. Phys. Lipids 134 (2005) 183–189.

[32] J.C. Dittmer, R.L. Lester, Simple, specific spray for the detection of phospholipids on the thin-layer chromatograms, J. Lipid Res. 5 (1964) 126–127.

[33] C.W.F. McClare, An accurate and convenient organic phosphorus assay, Anal. Biochem. 39 (1971) 527–530.

[34] M.R. Eftink, Fluorescence quenching reactions: probing biological macromolecular structure, in: T.G. Dewey (Ed.), Biophysical and Biochemical Aspects of Fluorescence Spectroscopy, Plenum Press, New York, 1991, pp. 1–41.

[35] J.R. Lakowicz, Principles of Fluorescence Spectroscopy, Plenum Press, New York, 1999.

[36] G.C. Chen, J.T. Yang, Two-point calibration of circular dichrometer with d-10-camphorsulfonic acid, Anal. Lett. 10 (1977) 1195–1207.

[37] A. Chattopadhyay, Exploring membrane organization and dynamics by the wavelength-selective fluorescence approach, Chem. Phys. Lipids 122 (2003) 3–17.

[38] H. Raghuraman, D.A. Kelkar, A. Chattopadhyay, Novel insights into membrane protein structure and dynamics utilizing the red edge excitation shift, in: C.D. Geddes, J.R. Lakowicz (Eds.), Reviews in Fluorescence 2005, vol. 2, Springer, New York, 2005, pp. 199–222.

[39] A.P. Demchenko, The red-edge effects: 30 years of exploration, Luminescence 17 (2002) 19–42.

[40] P. Mentré (Ed.), Water in the Cell, Cell. Mol. Biol., vol. 47, 2001, pp. 709–970.

[41] H. Raghuraman, S.K. Pradhan, A. Chattopadhyay, Effect of urea on the organization and dynamics of Triton X-100 micelles: a fluorescence approach, J. Phys. Chem., B 108 (2004) 2489–2496.

[42] S. Mukherjee, A. Chattopadhyay, Influence of ester and ether linkage in phospholipids on the organization and dynamics of the membrane interface: a wavelength-selective fluorescence approach, Langmuir 21 (2005) 287–293.

[43] S. Mukherjee, A. Chattopadhyay, Monitoring cholesterol organization in membranes at low concentrations utilizing the wavelength-selective fluorescence approach, Chem. Phys. Lipids 134 (2005) 79–84.

[44] S.S. Rawat, D.A. Kelkar, A. Chattopadhyay, Monitoring gramicidin conformations in membranes: a fluorescence approach, Biophys. J. 87 (2004) 831–843.

[45] D.A. Kelkar, A. Chattopadhyay, Effect of graded hydration on the dynamics of an ion channel peptide: a fluorescence approach, Biophys. J. 88 (2005) 1070–1080.

[46] A. Chattopadhyay, A. Arora, D.A. Kelkar, Dynamics of a membrane-bound tryptophan analog in environments of varying hydration: a fluorescence approach, Eur. Biophys. J. 35 (2005) 62–71.

[47] W. Qiu, L. Zhang, Y.-T. Kao, W. Lu, T. Li, J. Kim, G.M. Sollenberger, L. Wang, D. Zhong, Ultrafast hydration dynamics in melittin folding and aggregation: helix formation and tetramer self-assembly, J. Phys. Chem., B 109 (2005) 16901–16910.

[48] S.H. White, W.C. Wimley, Peptides in lipid bilayers: structural and thermodynamic basis of partitioning and folding, Curr. Opin. Struct. Biol. 4 (1994) 79–86.

[49] S. Mukherjee, A. Chattopadhyay, Wavelength-selective fluorescence as a novel tool to study organization and dynamics in complex biological systems, J. Fluoresc. 5 (1995) 237–246.

[50] J.M. Beechem, L. Brand, Time-resolved fluorescence of proteins, Annu. Rev. Biochem. 54 (1985) 43–71.

[51] E.P. Kirby, R.F. Steiner, The influence of solvent and temperature upon the fluorescence of indole derivatives, J. Phys. Chem. 74 (1970) 4480–4490.

[52] M.R. Eftink, L.A. Selvidge, P.R. Callis, A.A. Rehms, Photophysics of indole derivatives: experimental resolution of L_a and L_b transitions and comparison with theory, J. Phys. Chem. 94 (1990) 3469–3479.

[53] M.R. Eftink, Fluorescence quenching: theory and applications, in: J.R. Lakowicz (Ed.), Topics in Fluorescence Spectroscopy, vol. 2, Plenum Press, New York, 1991, pp. 53–126.

[54] A.S. Ladokhin, S.H. White, Folding of amphipathic α-helices on membranes: energetics of helix formation by melittin, J. Mol. Biol. 285 (1999) 1363–1369.

[55] Z. Szeltner, L. Polgar, Conformational stability and catalytic activity of HIV-1 protease are both enhanced at high salt concentration, J. Biol. Chem. 271 (1996) 5458–5463.

[56] J.M. Stevens, R.N. Armstrong, H.W. Dirr, Electrostatic interactions affecting the active site of class sigma glutathione *S*-transferase, Biochem. J. 347 (2000) 193–197.

[57] S.D. Manceva, M. Pusztai-Carey, P. Butko, Effect of pH and ionic strength on the cytolytic toxin Cyt1A: a fluorescence spectroscopy study, Biochim. Biophys. Acta 1699 (2004) 123–130.

[58] R.A. Bockmann, A. Hac, T. Heimburg, H. Grubmuller, Effect of sodium chloride on a lipid bilayer, Biophys. J. 85 (2003) 1647–1655.

[59] R. Kraayenhof, G.J. Sterk, H.W. Wong Fong Song, K. Krab, R.M. Epand, Monovalent cations differentially affect membrane surface properties and membrane curvature, as revealed by fluorescent probes and dynamic light scattering, Biochim. Biophys. Acta 1282 (1996) 293–302.

[60] J. Bigay, P. Gounon, S. Robineau, B. Antonny, Lipid packing sensed by ArfGAP1 couples COPI coat disassembly to membrane bilayer curvature, Nature 426 (2003) 563–566.